

Attention-guided Progressive Mapping for Profile Face Recognition

Junyang Huang
South China University of Technology
Guangzhou, China
eehjy1312@mail.scut.edu.cn

Changxing Ding*
South China University of Technology
Guangzhou, China
chxding@scut.edu.cn

Abstract

The past few years have witnessed great progress in the domain of face recognition thanks to advances in deep learning. However, cross pose face recognition remains a significant challenge. It is difficult for many deep learning algorithms to narrow the performance gap caused by pose variations; the main reasons for this relate to the intra-class discrepancy between face images in different poses and the pose imbalances of training datasets. Learning pose-robust features by traversing to the feature space of frontal faces provides an effective and cheap way to alleviate this problem. In this paper, we present a method for progressively transforming profile face representations to the canonical pose with an attentive pair-wise loss. First, to reduce the difficulty of directly transforming the profile face features into a frontal one, we propose to learn the feature residual between the source pose and its nearby pose in a block-by-block fashion, and thus traversing to the feature space of a smaller pose by adding the learned residual. Second, we propose an attentive pair-wise loss to guide the feature transformation progressing in the most effective direction. Finally, our proposed progressive module and attentive pair-wise loss are light-weight and easy to implement, adding only about 7.5% extra parameters. Evaluations on the CFP and CPLFW datasets demonstrate the superiority of our proposed method. Code is available at <https://github.com/hjy1312/AGPM>.

1. Introduction

Progress in deep learning has significantly advanced the face recognition techniques, such that the performance of many deep learning-based face recognition algorithms can be comparable or even superior to human performance. In spite of this, a recent study has demonstrated that the performance of many face recognition algorithms can drop by



Figure 1: Sample face images in different poses. The images in each row are from the same person but with different head poses. It can be observed that obvious intrinsic facial information discrepancy arises when a face gradually turns from frontal view to profile view.

over 10% from frontal-frontal to frontal-profile face verification [20], while this gap is much smaller for human performance. This indicates that large pose variation is still a challenge for the further advancement of face recognition, particularly in unconstrained environments.

There are two key reasons for the performance degradation caused by pose variation. First, intrinsic information discrepancy exists between the frontal and profile face images. As illustrated in Fig. 1, when the pose of face images change from frontal to profile, some parts of faces are exposed, while others are occluded, thus appearance and texture changes inevitably arise. This means that the information extracted from frontal faces and profile faces could be considerably different. Second, deep learning algorithms for face recognition usually suffer from pose imbalance problems in massive datasets, especially under real-world conditions. It can be quite expensive and infeasible to collect a large dataset with a relatively even pose distribution. Since deep learning is heavily data-driven [7, 5] and reliant on fitting the data, it is unsurprising that the algorithms trained on these pose-unbalanced datasets fit and generalize better on frontal face images than profile face images.

*Corresponding author

copyright not found ©null

A large number of promising works have been developed to address this problem. One primary research avenue is to synthesize face images across poses to reduce pose variation, including normalizing face images to the canonical pose [32, 18, 24] and augmenting training datasets by synthesizing face images across poses [33, 3]. However, due to self-occlusion and the complex backgrounds, the synthesized face images may be not sufficiently photorealistic. In contrast, some researchers have opted to tackle this problem in the feature space, including learning a unified pose-robust feature mapping [22, 1, 29] for face images at various poses and designing multiple pose specific models [16] to formulate different feature mappings for various poses. However, due to the high nonlinearity of pose variation, it is not easy to develop such a mapping that is capable of dealing with face images in all the poses. Moreover, if handling these poses separately, extra computational cost would introduce.

Accordingly, in this paper, we propose a progressive pose normalization framework, together with an attentive pair-wise loss to handle the pose variation problem by transforming features of the profile faces to frontal ones in a step by step manner. As indicated in [1], a gradual transition connection does exist between the profile and frontal face domains in the feature space. However, directly modeling the transformation from profile to frontal face might be problematic. As demonstrated in [12], pose variations change smoothly but nonlinearly along a latent manifold, directly transforming the features of extreme profile faces to those of frontal faces is a highly nonlinear process, which requires searching for the optimal point in a large search region and might be trapped into local minima. Meanwhile, multiple models are required to model these different nonlinear transformations at various poses. Instead, if we decompose the task into several smaller progressive tasks with pose transformation limited within a smaller interval, and ensure features in each interval possess similar properties, it would be much easier to achieve the goal. Inspired by these observations, we propose to model the nonlinear and complex transformation from extreme profile to frontal face by employing a progressive structure. More specifically, we roughly divide the pose into four groups and design three stacking transformation blocks. Each block will convert the feature of larger poses to that of its nearby poses, thus pose variation is narrowed down block by block.

We further introduce an attentive pair-wise loss (APL) to supervise this feature transformation process. For many cross pose face recognition algorithms [1, 18, 3], it is a natural choice to employ frontal face images as a strong supervision signal. Motivated by these works, we leverage the extracted features of frontal faces as the ground truth and penalize the L2 distance between them and the transformed features. However, we note that it may be too rigid to enforce the transformed feature to be completely the same as

the frontal ones owing to the intractable content discrepancy between profile and frontal faces. Instead, it would be better to focus only on maximizing their common elements in the deep feature space. As it is quite difficult to identify these common elements, we propose the following easier approach. Specifically, we apply features of frontal faces to generate an attention weights vector and then use them to modulate the L2 loss as a form of channel attention, which can capture the importance of each element in the feature vector. With the aid of these attention weights, our network focuses on pushing profile features to be closer to frontal ones in the most effective channels rather than all the channels, thus reducing the difficulty of frontalization and the possibility of overfitting to trivial parts.

We conduct extensive experiments on two popular benchmark datasets for cross-pose face recognition, i.e., CFP [20] and CPLFW [34]. The results show that our method consistently achieves superior performance for profile face recognition.

2. Related Works

Pose Robust Face Recognition. Enhancing algorithms' robustness to pose variation has long been a topic of interest in the field of face recognition. One main line of inquiry is based on image generation. For example, Qian et al. [18] introduced an unsupervised face normalization GAN model to transform a single face image of extreme pose into a canonical view. Zhao et al. [33] proposed synthesizing profile face images with a dual agent GAN framework for data augmentation. The drawback of these generative methods is that it can be quite difficult to synthesize sufficiently photorealistic face images due to the presence of occlusion and complex backgrounds. Another main research avenue is to learn a pose robust feature mapping. For example, Iacopo Masi et al. [16] proposed a pose-aware framework that incorporates multiple models for various poses. Cao et al. [1] introduced a Deep Residual Equivariant Mapping method to learn a residual between the features of profile faces and frontal ones. In comparison, our proposed methods are much more light-weight and easier to implement, increasing the total number of parameters by only 7.5% across the whole network, while also being more effective for profile face recognition.

Loss Functions for Face Recognition. Loss functions plays a key role in face recognition tasks. A large proportion of these functions are the variants of the classic cross entropy loss, including SphereFace [13], CosFace [25] and ArcFace [4], et al. These loss functions tend to minimize the intra-class distance and maximize inter-class distance by constraining the classification decision boundary. Another mainstream approach is pair-wise loss. This approach aims at enhancing the compactness and discriminative power of extracted features by intuitively forming pairs

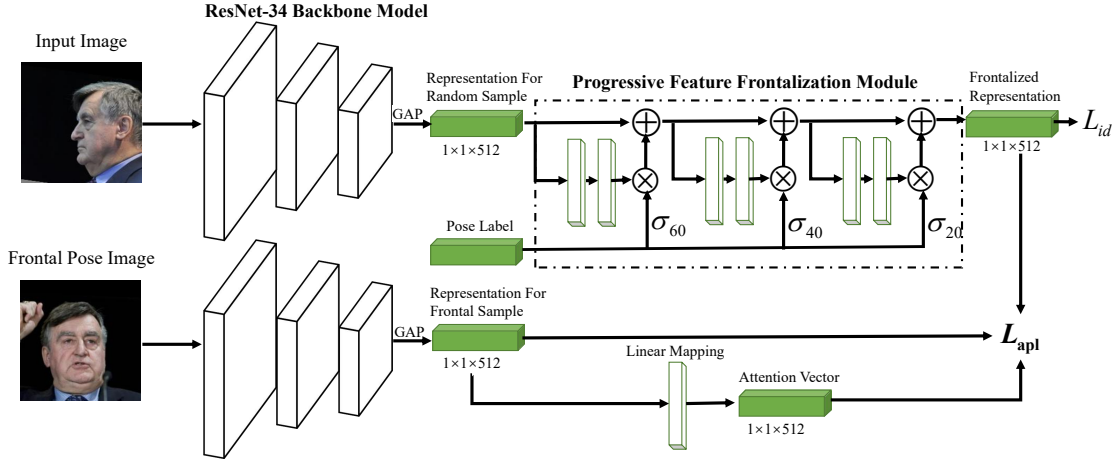


Figure 2: An overview of our proposed approach. First, each training sample and its assigned frontal face image of the same identity are fed to the ResNet-34 backbone to produce two feature embeddings. Second, progressive frontalization in the feature space are performed to map the feature embeddings into frontal feature space according to the pose of each image. Finally, with the modulation of an attention vector generated from the feature embedding of the assigned frontal face, identity classification loss and attentive pair-wise loss are utilized to train the entire network.

to train. For example, contrastive loss [2] directly optimizes the Euclidean distance between similar and dissimilar pairs in Siamese networks. Triplet loss [19] takes triplets as inputs and adds a margin between positive pairs and negative pairs to reduce inter-class distance while increasing outer-class distance. Nevertheless, in contrast to our proposed attentive pair-wise loss, which focuses on alleviating extreme pose discrepancy to facilitate unconstrained face recognition, none of these loss functions explicitly aim at handling the pose variation problem.

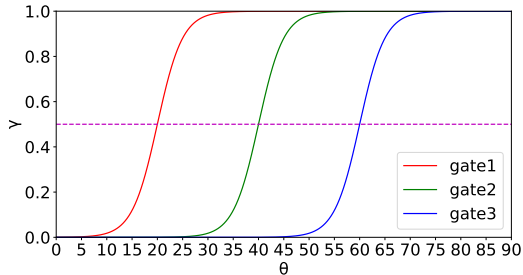


Figure 3: A visualization of the soft-gate mapping for the progressive blocks. The horizontal axis represents the value of the yaw angle θ , while the vertical axis represents the soft gate coefficient $\gamma(\theta_i, \theta)$.

3. Method

In this paper, we propose a progressive feature frontalization framework together with an attentive pair-wise loss for cross-pose face recognition. Fig. 2 presents an overview of our proposed method.

3.1. Progressive Frontalization in Feature Space

To begin with, we introduce the problem formulation. As illustrated in Fig. 2, a face image x_s and its accommodated frontal ground truth image x_f are fed to the face recognition backbone to extract two deep feature embeddings, $\psi(x_s)$ and $\psi(x_f)$, where the face recognition backbone is denoted as a mapping function ψ . Our goal is to force $\psi(x_s)$ to approach the feature space of frontal faces to the greatest extent through our proposed progressive module.

In the interests of clarity, we assume that face poses are divided into four bins within $[0^\circ, 90^\circ]$ according to the absolute values. Face images of $[0^\circ, 20^\circ]$, $[20^\circ, 40^\circ]$, $[40^\circ, 60^\circ]$ and $[60^\circ, 90^\circ]$ are respectively denoted as frontal face, half frontal face, half profile face and profile face, respectively.

In our method, each progressive block specifies a certain nonlinear feature transformation between a pose bin and its nearby bin. For illustrative purposes, we term the three blocks respectively as profile to half profile block, half profile to half frontal block, and half frontal to frontal block in sequence. Each block takes the output of the last block as input, and then maps the features at a larger pose to virtual features at its nearby pose, or simply performs an identity mapping when the pose of the current input is smaller than the target pose of the block.

Similar to [1, 26, 6], we utilize the residual block of our backbone as the basic architecture of the transformation model; however, we opt to replace the 3×3 convolutions with 1×1 convolutions and incorporate soft gates into these blocks, facilitating the adaptive performing of suitable transformations for different poses. More specifically, each progressive block attempts to learn a residual between fea-

tures from a larger pose to its nearby pose, which is then modulated by the pre-calculated soft gate coefficient and plus the original features to formulate the features of the target pose. We denote these residual blocks respectively as R_i ($i = 1, 2, 3$), while the soft gate mapping is denoted as $\gamma(\theta_i, \theta)$; subsequently, the output of each progressive block is formulated as bellow:

$$f_i(x) = f_{i-1}(x) + \gamma(\theta_i, \theta)R_i(f_{i-1}(x)). \quad (1)$$

The coefficient $\gamma(\theta_i, \theta)$ serves as a selecting gate for the features that pass through each progressive block. This coefficient in the range of $[0.0, 1.0]$ determines the amount of the learning residual for the input feature of each block. Given the features of a face image at the pose θ as input, each block compares θ with its preset threshold pose value θ_i ($\theta_i = 60^\circ, 40^\circ, 20^\circ$), then produces a soft gate coefficient accordingly, as follows:

$$\gamma(\theta_i, \theta) = \frac{1}{1 + e^{-10(\theta/\theta_i - 1)}}. \quad (2)$$

As shown in Fig. 3, this formula can be also conceived as a soft binary mapping. When θ is slightly larger than θ_i , the soft gate coefficient will quickly saturate to 1.0; moreover, when θ is slightly smaller than θ_i , this coefficient quickly decrease to 0. It is noteworthy that as the pose variation changes nonlinearly but smoothly, it would be unsuitable to directly employ a step function for mapping. Instead, a transition zone is necessary when θ approximates θ_i . Taking this into account, we employ the soft gate mapping function presented above to control whether the blocks conduct frontalization transform or directly perform an identity mapping.

3.2. Attentive Pair-wise Loss

To calculate the attentive pair-wise loss, we first assign a frontal face image of the same identity for each input face image. Each input face image x_s and its accommodated frontal face image x_f are passed through the same backbone model ResNet-34 and formulated feature embedding as $\psi(x_s)$ and $\psi(x_f)$ respectively. As discussed above, it is difficult to determine the potential common elements in the embeddings of the image pair when pose difference is large, as the extracted features of such profile face images tend to be less discriminative. However, and notably, most common elements of the frontal-profile face image pair have strong responses in the feature embedding of frontal faces. Thus, we formulate the attentive weighting vectors as follows:

$$A(x_f) = \frac{\text{abs}(\psi(x_f))}{\max(\text{abs}(\psi(x_f)))}, \quad (3)$$

where $\text{abs}(\cdot)$ represents the element-wise absolute value of a vector, and $\max(\cdot)$ returns the largest element in a vector.

With the frontalized feature embedding of profile face denoted as $F(\psi(x_s))$, the proposed attentive pair-wise loss can be calculated as follows:

$$L_{apl} = \frac{1}{N} \sum_{i=1}^N \|(F(\psi(x_s^i)) - \psi(x_f^i)) \odot A(\psi(x_f^i))\|_2^2, \quad (4)$$

where N denotes the batch size, while \odot represents the element-wise multiplication operation.

During training, we combine the cross entropy loss for identity classification and the above attentive pair-wise loss together to train the entire network end to end. The overall loss function can be expressed as follows:

$$L = L_{id} + \lambda L_{apl}, \quad (5)$$

where λ is a hyper parameter used to balance the cross entropy loss and the attentive pair-wise loss.

4. Experiments

4.1. Datasets and Evaluation Metrics

CFP is a challenging in-the-wild dataset that focuses on face verification from frontal to extreme head poses [20]. It consists of 500 celebrities, with 10 frontal face images and four profile face images for each person. In the standard protocol, the whole dataset is split into 10 folds, each of which contains 350 intra-class pairs and 350 inter-class pairs, with the same number of frontal-frontal and frontal-profile pairs. Accuracy, Equal Error Rate (EER) and Area Under Curve (AUC) metrics are then estimated by conducting 10-fold cross validation.

CPLFW is reorganized from the LFW dataset [9] by searching and selecting 3000 positive pairs with large pose difference to emphasize intra-class pose variation, meanwhile also eliminating race and gender differences between 3000 negative pairs [34]. The evaluation on CPLFW is based on the official protocol, i.e. 10-fold cross validation, with 300 positive pairs and 300 negative pairs for each fold.

4.2. Implementation Details

Training Data. We separately employ a subset of the MS-Celeb-1M [7] database and a refined clean version of MS-Celeb-1M proposed by [4] as our training data, in order to facilitate fair comparisons with other methods. To create the first subset, we sampled 2,179,216 face images from 62,338 identities in the original MS-Celeb-1M dataset, while the refined clean version contains 5,193,691 face images of 93,436 identities. Moreover, in the interests of fair comparison, we have removed the images of identities that overlap with the testing datasets.

Data Preprocessing. We perform standard preprocessing on both the training datasets and testing datasets. First, we detect the face bounding boxes and five facial landmarks

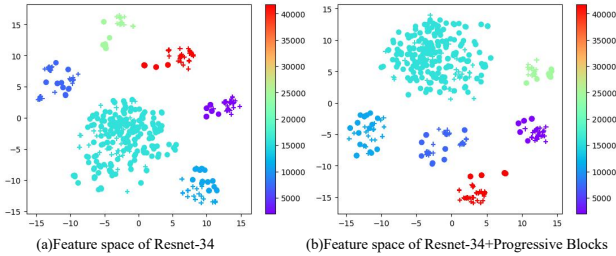


Figure 4: Visualization of feature cluster used TSNE(best view with zoom in). Here we use solid dots • to represent frontal faces and symbols + to denote profile faces. Different colors are used to represent different subjects. (a) Feature space of the baseline, i.e. ResNet-34. (b) Embeddings obtained by ResNet-34 with the progressive blocks. It is shown that the feature clusters become more compact despite of pose variations.

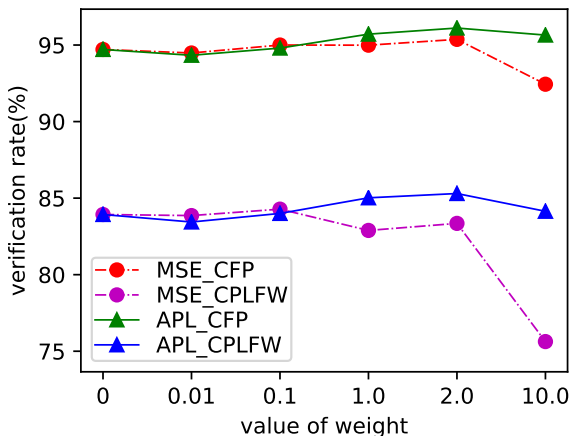


Figure 5: Comparison in verification accuracy between APL and plain MSE with different weights.

with MTCNN [30] for each face image. We then crop the faces with the detected boxes, align them with five facial landmarks (the two eye centers, the nose tip and both mouth corners), and resize to 230×230 pixels. Meanwhile, we adopt the tool in [14] to estimate the yaw angles of the face images. Besides, common data augmentation methods are utilized to reduce over-fitting in the training stage, i.e. random gray scaling, random horizontal flipping, and random cropping.

Training Setting. Our framework is implemented in Pytorch. We train our network on two NVIDIA TITAN V GPUs with a batch size of 200. To construct a mini-batch for training, we first randomly sample face images from the training set, and then respectively sample a frontal face image with a pose absolute value smaller than 10° as the ground truth for each of them. For face images for which no such frontal face image is available, we simply employ face

images with the same identity and the smallest pose as their ground truth. Next, the standard stochastic gradient descent (SGD) optimizer, with a weight decay of 5×10^{-4} and a momentum of 0.9, is utilized to train the entire network. The initial learning rate is set to 0.1. The total number of training epochs is 30, and the epoch milestones are 5, 10, 15 and 20. When the epoch reaches a milestone, the learning rate decays by a factor of 0.5, 0.2, 0.1 and 0.1, respectively.

4.3. Ablation Study

4.3.1 Effectiveness of progressive blocks

We first study the effectiveness of the progressive blocks. The results are presented in Table 1. It can be observed that the progressive module alone does not consistently boost the performance on both datasets. This might be due to the lack of strong supervision such as MSE or APL, which would help the network gain insight into how to drag the profile faces closer to the frontal faces in the deep feature space. In fact, ‘MSE + progressive’ and ‘APL + progressive’ outperform the ‘MSE-only’ and ‘APL-only’ settings, respectively. Through visualizing the deep feature space of the baseline ResNet-34 and ResNet-34 with the progressive blocks via t-SNE in Fig. 4, we can observe that the progressive blocks help formulate more compact feature cluster in spite of pose variations. These experimental results strongly verify the effectiveness of our progressive module on face recognition across poses.

Next, we adopt ‘MSE-only’ as the baseline and conduct an experiment on the number of progressive blocks with different pose splitting strategies and employ different amounts of progressive blocks. We divide the face images into two groups (with the pose value within $[0^\circ, 45^\circ]$ and $[45^\circ, 90^\circ]$), three groups ($[0^\circ, 25^\circ]$, $[25^\circ, 55^\circ]$, $[55^\circ, 90^\circ]$) and four groups ($[0^\circ, 20^\circ]$, $[20^\circ, 40^\circ]$, $[40^\circ, 60^\circ]$, $[60^\circ, 90^\circ]$). These splitting strategies respectively correspond to one block, two blocks and three blocks, which share the same basic architecture. The results in Table 2 demonstrate that it is more effective to segment the pose space and progressively process face images of different poses.

Finally, to further verify the effectiveness of the progressive module, we remove the soft-gate methodology and let $\gamma(\theta_i, \theta) = 1.0$, keeping the same parameters compared to our progressive module. It can be observed from Table 3 that our progressive module achieves better performance. This indicates that the performance promotion in our approach is not simply due to the increase of model complexity; instead, it is a result of the mechanism that splits the pose space and processes each pose segment in a different manner.

4.3.2 Effectiveness of APL

To investigate the effectiveness of our proposed attentive pair-wise loss, we first conduct a qualitative analysis. We

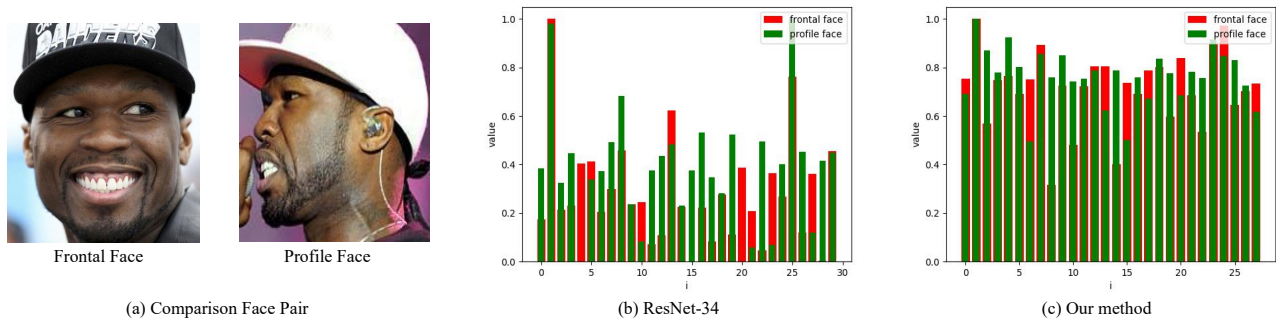


Figure 6: A visualization of the maximum elements in feature embeddings of a frontal face and a profile face. Red bars represent elements for the frontal face, while green bars represent the elements for the profile face. (a) Selected frontal and profile face images. (b) Visualization of the embeddings extracted by the raw ResNet-34 model trained with only necessary classification loss. This indicates that feature embeddings between the frontal-profile face pairs not only share the common elements but also have their unique parts. (c) Visualization of our method, which significantly boosts the excavation of potential common elements across poses.

Dataset	MSE	Prog.	APL	CFP	CPLFW
Ms-Subset	-	-	-	94.71 ± 1.56	83.93 ± 1.96
	✓	-	-	94.99 ± 1.20	82.89 ± 2.41
	-	✓	-	94.33 ± 1.63	83.99 ± 2.20
	-	-	✓	96.11 ± 1.15	84.41 ± 2.52
	✓	✓	-	95.65 ± 0.86	83.63 ± 2.31
	-	✓	✓	96.11 ± 1.04	85.30 ± 2.05
Ms-Refined	-	-	-	97.55 ± 0.59	87.47 ± 1.61
	✓	-	-	97.83 ± 0.67	86.93 ± 1.65
	-	✓	-	97.82 ± 0.76	88.64 ± 1.37
	-	-	✓	98.25 ± 0.54	88.69 ± 1.83
	✓	✓	-	98.00 ± 0.51	87.42 ± 1.71
	-	✓	✓	98.44 ± 0.40	89.37 ± 1.87

Table 1: Ablation study on the progressive module and APL. The frontal-profile face verification accuracy on the CFP dataset and face verification accuracy on the CPLFW dataset are reported here.

Method	CFP	CPLFW
Baseline	94.99 ± 1.20	82.89 ± 2.41
One block	95.29 ± 0.94	83.26 ± 2.09
Two block	95.11 ± 0.98	83.55 ± 2.40
Three block	95.65 ± 0.86	83.63 ± 2.31

Table 2: Ablation study on the number of blocks in the progressive module. Results include the frontal-profile face verification accuracy on the CFP dataset and face verification accuracy on the CPLFW dataset

randomly select a frontal face image and profile face image with the same identity from the CFP dataset, then visualize their respective feature embeddings from the raw ResNet-

Gate setting	Accuracy	EER
Baseline	94.99 ± 1.20	4.83 ± 1.15
fixed $\gamma(\theta_i, \theta) = 1.0$	95.34 ± 1.08	4.27 ± 1.09
unfixed	95.65 ± 0.86	3.91 ± 0.93

Table 3: Ablation study on soft-gates. Accuracy and EER metrics of face verification on the CFP dataset are reported.

34 model and our proposed method. We only consider the statistically top 20 maximum values in the 512-dim feature vector, as these represent the most effective activation. The results in Fig. 6 reveal that our proposed attentive pair-wise loss helps to boost the excavation of potential common activation across poses.

Method	Training Data	Backbone	CFP-FP(%)
Sengupta et al. [20]	CA(0.49M)	DCNN(1.7M)	84.91
PIM [32]	MS(10M)	LightCNN(8.4M)	93.10
DR-GAN [24]	CA+MP(0.5M)	DCNN(13.0M)	93.41
PFE [21]	MS(4.4M)	ResNet64(19.3M)	93.34
Peng et al. [17]	CA+MP(0.5M)	CASIA-Net(1.7M)	93.76
UV-GAN [3]	MS(4M)	ResNet27(35.1M)	94.05
Yin et al. [29]	CA(0.49M)	p-CNN(1.8M)	94.39
ArcFace [4]	MS(5.8M)	ResNet50(160.0M)	95.56
Wang et al. [28]	MS(3.28M)	AttentionNet(89.3M)	95.7
CircleLoss [23]	MS(3.6M)	ResNet34(21.3M)	96.02
CurricularFace [10]	MS(5.8M)	ResNet100(248.0M)	98.37
Our Method with MS subset			
ResNet-34	MS(2.2M)	ResNet34(21.3M)	94.71
Our method	MS(2.2M)	ResNet34(22.9M)	96.11
Our Method with Refined MS			
ResNet-34	MS(5.2M)	ResNet34(21.3M)	97.55
Our method	MS(5.2M)	ResNet34(22.9M)	98.4

Table 4: Comparisons in terms of frontal-profile verification accuracy on the CFP dataset. For the training data, we denote Ms-Celeb-1M, CASIA-WebFace, Multi-PIE as MS, CA and MP, respectively.

Method	Training Data	Backbone	Accuracy(%)
ML [31]	MS(7.03M)	MobileFaceNet(1.1M)	82.44
MN [11]	MS(7.03M)	MobileFaceNet(1.1M)	83.49
DC [15]	MS(7.03M)	MobileFaceNet(1.1M)	84.01
CT [8]	MS(7.03M)	MobileFaceNet(1.1M)	84.83
Co-Mining [27]	MS(7.03M)	MobileFaceNet(1.1M)	85.70
Zhong et al. [35]	CA(0.67M)	ResNet50(43.6M)	88.22
ArcFace [4, 28]	MS(3.28M)	AttentionNet(89.3M)	88.78
Wang et al. [28]	MS(3.28M)	AttentionNet(89.3M)	89.69
CurricularFace [10]	MS(5.8M)	ResNet100(248.0M)	93.13
Our Method with MS subset			
ResNet-34	MS(2.2M)	ResNet34(21.3M)	83.93
Our method	MS(2.2M)	ResNet34(22.9M)	85.30
Our Method with Refined MS			
ResNet-34	MS(5.2M)	ResNet34(21.3M)	87.47
Our method	MS(5.2M)	ResNet34(22.9M)	89.37

Table 5: Verification accuracy comparison on the CPLFW dataset. For the training data, we denote Ms-Celeb-1M, CASIA-WebFace, VGGFace2 respectively as MS, CA and VF2.

We then compare the performances of traditional MSE loss and our proposed attentive pair-wise loss. The progressive module is removed to facilitate clean comparison. Following Eq. 5, MSE loss and APL are respectively combined with the cross entropy loss to train the backbone model with the same settings. As is clear from the results in Table 1, our attentive pair-wise loss can significantly improve the face recognition performance compared to the MSE loss. We further embed the progressive module into the entire network. The results in Table 1 show that the APL+Progressive setting yields the highest performance, outperforming the MSE+Progressive setting.

4.3.3 An Ablation Study on Balancing Parameters

In this experiment, we study the effect of different parameters to balance the cross-entropy loss and the pair-wise loss in Eq. 5. We carefully examine the possible parameters and assign the following weights to the pair-wise losses: 0.01, 0.1, 0, 1, 2, and 10. We calculate the verification ac-

curacy on both the CFP and CPLFW datasets and present the results in Fig. 5. From the results, we can make the following observations: First, the optimal balancing parameter for MSE loss is about 1.0, while that for our attentive pair-wise loss is about 2.0. This can be explained by the fact that each element in the attention vector for APL is actually smaller than 1.0 after maximum normalization; Therefore, the weight should be correspondingly somewhat larger. Second, the best performance of our APL is significantly superior to all the settings of the MSE. This experiment provides further evidence for the superior performance of APL.

4.4. Comparisons with SOTA Methods

Results on CFP Table 4 presents the performance of recent methods on the CFP dataset, which covers almost all the categories of methods for face recognition across poses discussed above. From the table we can observe that our proposed method significantly boosts the face verification performance compared with the raw ResNet-34

model and surpasses that of the most recent methods reported above. Notably, although our model is trained using a relatively smaller training set, it still outperforms the CircleLoss [23], which adopts the same backbone as our method but uses a much larger training set. Furthermore, after we re-implement our method on a larger training set (the refined version of Ms-Celeb-1M), we achieve higher performance than state-of-the-art methods, even though our backbone model is far more light-weight.

Results on CPLFW Similar to the testing protocol on CFP, we follow the official 10-fold cross validation protocol and test it on the CPLFW dataset. We report the face verification accuracy and provide a comparison with recent methods in Table 5. As can be seen from the table, our method achieves impressive improvement compared with the raw ResNet-34 model: specifically, 1.37% accuracy improvement on the subset of Ms-Celeb-1M and 1.9% accuracy improvement on the refined version of Ms-Celeb-1M. When compared with other methods, it can further be observed that our method is superior to most of the above methods. If we were to implement our method with a superior backbone and a larger-scale training set, it would achieve better performance.

5. Conclusion

In this paper, we proposed a novel light-weight progressive module to model the nonlinear transformation from arbitrary faces to frontal faces in the feature space. Our progressive module is not only effective in bridging the gap between the profile faces and frontal faces, but can also flexibly cope with faces across various poses. Furthermore, we also introduce an attentive pair-wise loss to guide the feature transformation progressing in the most effective direction. Our method is light weight and easy to implement, increasing overall computational cost by only a small amount. Experiments on the CFP and CPLFW datasets demonstrate that our proposed methods consistently brings significant performance promotion for face recognition across poses.

6. Acknowledgement

This work was supported by the National Natural Science Foundation of China under Grant 61702193, and the Fundamental Research Funds for the Central Universities of China under Grant 2019JQ01.

References

- [1] K. Cao, Y. Rong, C. Li, X. Tang, and C. C. Loy. Pose-robust face recognition via deep residual equivariant mapping. In *CVPR*, pages 5187–5196, 2018. 2, 3
- [2] S. Chopra, R. Hadsell, and Y. LeCun. Learning a similarity metric discriminatively, with application to face verification. In *CVPR*, volume 1, pages 539–546 vol. 1, 2005. 3
- [3] J. Deng, S. Cheng, N. Xue, Y. Zhou, and S. Zafeiriou. Uv-gan: Adversarial facial uv map completion for pose-invariant face recognition. In *CVPR*, pages 7093–7102, 2018. 2, 7
- [4] J. Deng, J. Guo, N. Xue, and S. Zafeiriou. Arcface: Additive angular margin loss for deep face recognition. In *CVPR*, pages 4685–4694, 2019. 2, 4, 7
- [5] C. Ding and D. Tao. A comprehensive survey on pose-invariant face recognition. *ACM TIST*, 7(3):1–42, 2016. 1
- [6] C. Ding, K. Wang, P. Wang, and D. Tao. Multi-task learning with coarse priors for robust part-aware person re-identification. *TPAMI*, pages 1–1, 2020. 3
- [7] Y. Guo, L. Zhang, Y. Hu, X. He, and J. Gao. Ms-celeb-1m: Challenge of recognizing one million celebrities in the real world. *Electronic Imaging*, 2016:1–6, 2016. 1, 4
- [8] B. Han, Q. Yao, X. Yu, G. Niu, M. Xu, W. Hu, I. Tsang, and M. Sugiyama. Co-teaching: Robust training of deep neural networks with extremely noisy labels. In *NIPS*, pages 8527–8537, 2018. 7
- [9] G. Huang, M. Ramesh, T. Berg, and E. Learned-Miller. Labeled faces in the wild: A database for studying face recognition in unconstrained environments. *Tech. rep.*, 10 2008. 4
- [10] Y. Huang, Y. Wang, Y. Tai, X. Liu, P. Shen, S. Li, J. Li, and F. Huang. Curricularface: Adaptive curriculum learning loss for deep face recognition. In *CVPR*, pages 5900–5909, 2020. 7
- [11] L. Jiang, Z. Zhou, T. Leung, L.-J. Li, and L. Fei-Fei. Mentornet: Learning data-driven curriculum for very deep neural networks on corrupted labels. In *ICML*, 2018. 7
- [12] M. Kan, S. Shan, H. Chang, and X. Chen. Stacked progressive auto-encoders (spae) for face recognition across poses. In *CVPR*, pages 1883–1890, 2014. 2
- [13] W. Liu, Y. Wen, Z. Yu, M. Li, B. Raj, and L. Song. Spheraface: Deep hypersphere embedding for face recognition. In *CVPR*, pages 6738–6746, 2017. 2
- [14] G. Luo. head-pose-estimation-and-face-landmark, 2016. 5
- [15] E. Malach and S. Shalev-Shwartz. Decoupling “when to update” from “how to update”. In *NIPS*, pages 960–970, 2017. 7
- [16] I. Masi, F. Chang, J. Choi, S. Harel, J. Kim, K. Kim, J. Leksut, S. Rawls, Y. Wu, T. Hassner, W. AbdAlmageed, G. Medioni, L. Morency, P. Natarajan, and R. Nevatia. Learning pose-aware models for pose-invariant face recognition in the wild. *TPAMI*, 41(2):379–393, 2019. 2
- [17] X. Peng, X. Yu, K. Sohn, D. N. Metaxas, and M. Chandraker. Reconstruction-based disentanglement for pose-invariant face recognition. In *ICCV*, pages 1632–1641, 2017. 7
- [18] Y. Qian, W. Deng, and J. Hu. Unsupervised face normalization with extreme pose and expression in the wild. In *CVPR*, pages 9843–9850, 2019. 2
- [19] F. Schroff, D. Kalenichenko, and J. Philbin. Facenet: A unified embedding for face recognition and clustering. In *CVPR*, pages 815–823, 2015. 3
- [20] S. Sengupta, J. Chen, C. Castillo, V. M. Patel, R. Chellappa, and D. W. Jacobs. Frontal to profile face verification in the wild. In *WACV*, pages 1–9, 2016. 1, 2, 4, 7

- [21] Y. Shi and A. Jain. Probabilistic face embeddings. In *ICCV*, pages 6901–6910, 2019. 7
- [22] Y. Shi, X. Yu, K. Sohn, M. Chandraker, and A. K. Jain. Towards universal representation learning for deep face recognition. In *CVPR*, pages 6816–6825, 2020. 2
- [23] Y. Sun, C. Cheng, Y. Zhang, C. Zhang, L. Zheng, Z. Wang, and Y. Wei. Circle loss: A unified perspective of pair similarity optimization. In *CVPR*, pages 6397–6406, 2020. 7, 8
- [24] L. Tran, X. Yin, and X. Liu. Disentangled representation learning gan for pose-invariant face recognition. In *CVPR*, pages 1283–1292, 2017. 2, 7
- [25] H. Wang, Y. Wang, Z. Zhou, X. Ji, D. Gong, J. Zhou, Z. Li, and W. Liu. Cosface: Large margin cosine loss for deep face recognition. In *CVPR*, pages 5265–5274, 2018. 2
- [26] K. Wang, C. Ding, S. J. Maybank, and D. Tao. Cdpm: Convolutional deformable part models for semantically aligned person re-identification. *TIP*, 29:3416–3428, 2020. 3
- [27] X. Wang, S. Wang, H. Shi, J. Wang, and T. Mei. Co-mining: Deep face recognition with noisy labels. In *ICCV*, pages 9357–9366, 2019. 7
- [28] X. Wang, S. Zhang, S. Wang, T. Fu, H. Shi, and T. Mei. Misclassified vector guided softmax loss for face recognition. In *AAAI*, pages 12241–12248, 2020. 7
- [29] X. Yin and X. Liu. Multi-task convolutional neural network for pose-invariant face recognition. *TIP*, 27(2):964–975, 2018. 2, 7
- [30] K. Zhang, Z. Zhang, Z. Li, and Y. Qiao. Joint face detection and alignment using multitask cascaded convolutional networks. *IEEE Signal Processing Letters*, 23(10):1499–1503, 2016. 5
- [31] Y. Zhang, T. Xiang, T. M. Hospedales, and H. Lu. Deep mutual learning. In *CVPR*, pages 4320–4328, 2018. 7
- [32] J. Zhao, Y. Cheng, Y. Xu, L. Xiong, J. Li, F. Zhao, K. Jayashree, S. Pranata, S. Shen, J. Xing, S. Yan, and J. Feng. Towards pose invariant face recognition in the wild. In *CVPR*, pages 2207–2216, 2018. 2, 7
- [33] J. Zhao, L. Xiong, P. Karlekar Jayashree, J. Li, F. Zhao, Z. Wang, P. Sugiri Pranata, P. Shengmei Shen, S. Yan, and J. Feng. Dual-agent gans for photorealistic and identity preserving profile face synthesis. In *NIPS*, pages 66–76, 2017. 2
- [34] T. Zheng and W. Deng. Cross-pose lfw: A database for studying cross-pose face recognition in unconstrained environments. Technical Report 18-01, Beijing University of Posts and Telecommunications, February 2018. 2, 4
- [35] Y. Zhong, W. Deng, M. Wang, J. Hu, J. Peng, X. Tao, and Y. Huang. Unequal-training for deep face recognition with long-tailed noisy data. In *CVPR*, pages 7804–7813, 2019. 7